Effect of non-ionic surfactants on transient cavitation in a megasonic field

M. Keswani *, S. Raghavan, P. Deymier

Department of Materials Science and Engineering, The University of Arizona, 1235 E James E Rogers Way, Tucson, AZ 85721, USA

ARTICLE INFO

ABSTRACT

High resolution chronoamperometry has been used to characterize the effect of two non-ionic surfactants, Triton® X-100 and NCW®-1002, on cavitation in aqueous solutions exposed to ~1 MHz sound field. Specifically, using ferricyanide as the electroactive species, temporal variation of current during its reduction on a 25 μm Pt microelectrode has been measured and is used to elucidate transient cavity behavior. The chronoamperograms for solutions exposed to megasonic field show current 'peaks' riding on the baseline current. These current 'peaks' have been attributed to the diffusion of ferricyanide species concentrated at the liquid–vapor interface of a transient cavity at the end of its collapse. In the presence of surfactants, the frequency of occurrence of current 'peaks' with magnitude $\geqslant 0.3$ μA is found to increase indicating a higher number of transient cavity collapses. A simple mathematical model based on diffusion developed previously by the authors has been used to extract the maximum cavity size and range of distances between the center of the collapsing cavity and the electrode surface in the surfactant solutions.

© 2012 Elsevier B.V. All rights reserved.

1. Introduction

Particle contamination is a major cause of yield loss in the fabrication of integrated circuits. Megasonic (~1 MHz frequency) assisted wet cleaning has been of interest to the semiconductor industry due to its effectiveness in removing particulate contaminants from silicon wafer surfaces [1]. Chemical systems such as dilute ammonium hydroxide–hydrogen peroxide solutions (1NH$_4$OH (28%):1H$_2$O$_2$ (30%):100H$_2$O by volume), when used in conjunction with applied megasonic field provide the advantage of reduced chemical consumption while preserving high particle removal efficiency (PRE). Acoustic streaming and cavitation are understood to be the primary mechanisms for particle removal during megasonic cleaning [2]. The different variables that can affect acoustic streaming and cavitation include sound field parameters (frequency, power density and percent duty cycle) and solution parameters (temperature, dissolved gas content, and type of liquid). Surfactants are commonly used as additives in megasonic cleaning as they enhance the cleaning efficiency by improving the wettability of the surface and reducing particle re-deposition by changing the interfacial charging behavior of the surface and particles [3]. Since, surfactants are known to preferentially adsorb at gas/liquid and solid/liquid interface and reduce the liquid surface tension, they can be expected to affect cavitation behavior in a megasonic field.

Although there have been many studies investigating acoustic bubble cavitation, there is limited literature on the effect of surfactants on bubble activity [4]. Surfactants can affect cavitation in many ways: (i) by altering the coalescence between bubbles through surface adsorption, which has an impact on size distribution of the cavitating bubbles and eventually on their transformation to stable or transient cavities, (ii) through increase in rectified diffusion by allowing more gas to enter inside the bubble during expansion than it leaves during compression [5], and (iii) possible enhancement in microstreaming due to no slip boundary layer condition generated at the bubble surface by adsorption of surfactant [6].

One of the early studies on examining the effect of surface active solutes on bubble coalescence in aqueous solution was conducted by Oolman and Blanch using a microscope and a high speed camera [7]. It was found that the extent of coalescence between air bubbles was inhibited by the adsorption of surface active solutes such as linear aliphatic alcohols and n-butyric acid. Crum measured the growth of acoustically cavitating bubbles in air saturated aqueous solutions containing different levels of ethoxylated octyl-phenol (Photoflo®) surfactant at 25 °C [6,8]. The growth rate of 50 μm bubble, as measured using a microscope, increased from 10 to 100 nm/s with reduction in liquid surface tension from 65 to 30 mN/m. The effect was attributed to reduction in threshold pressure amplitude for rectified diffusion with decrease in liquid surface tension.

Measurements of acoustic emission and sonoluminescence (SL) from a *single* air bubble (radius of 9 μm) in degassed water irradiated with 16.5 kHz have been reported in the presence and absence of Triton® X-100 surfactant [9]. Acoustic and SL measurements were made using a needle hydrophone and photomultiplier tube (PMT). Reduction in both acoustic output and SL signal was

observed for Triton® X-100 surfactant at a concentration of 0.1 CMC (critical micelle concentration) in DI water. At higher concentrations of 0.25 CMC and CMC, the bubble was unstable and exhibited erratic behavior with weak or no acoustic and SL emissions.

Sunartio et. al., investigated the effect of aliphatic alcohols and sodium dodecyl sulfate (SDS) on extent of bubble coalescence for various frequencies (∼200–1000 kHz) and power densities (0.9–1.6 W/cm²) in aqueous solutions [10]. The bubble coalescence was determined from change in liquid volume measured using capillary rise method. It was observed that adsorption of surface active solutes retarded bubble coalescence at all frequencies and power levels. The effect of SDS on acoustic cavitation activity in air saturated aqueous solution at 20 °C has been investigated using hydrophone based passive cavitation detection technique and sonoluminescence measurements [11]. The study was conducted at different acoustic pulse lengths (0–2500 cycles) for sound frequencies of ∼0.52 and 1.0 MHz and transducer powers of 0–100 W. A decrease in SL intensity was observed when the surfactant concentration was lower than ∼1.6 mM for short pulse cycles. It was suggested that coalescence of bubbles was retarded by SDS, which resulted in a higher population of smaller bubbles that dissolved away during transducer off time for short pulse cycles. Increase in SDS concentrations from 1.6 to 4 mM resulted in enhanced SL signal due to improvement in the growth rate of bubbles by rectified diffusion that presumably led to population of larger bubbles which survived during the transducer off time.

In order to understand the behavior of cavitating bubbles during actual wafer cleaning conditions, it is important to probe activity of a single bubble close to a solid surface that is generated acoustically and is cavitating in a multibubble cavitation environment. In this context, high resolution microelectrode based electrochemical measurements can be extremely useful. As bubbles cavitate in a sound field, they induce a flux of material in the liquid. An electrically biased electrode in close vicinity of the bubbles will detect this flux in the form of induced current, provided an electroactive species (e.g. potassium ferricyanide) is present in the solution. A microelectrode would allow monitoring of the activity of a single bubble close to a solid boundary. Additionally, since cavitating bubbles exhibit different behaviors such as oscillations and collapse in microsecond to millisecond time scale, high (time) resolution measurements of current can be used to capture cavitation details [12].

In this work, the effect of two high purity non-ionic surfactants commonly used for wafer cleaning on single bubble activity in 1 MHz sound frequency has been characterized using high resolution chronoamperometry (current vs. time at a constant potential) measurements. The two surfactants that were used are 4-(1,1,3,3-Tetramethylbutyl)phenyl-polyethylene glycol (Triton® X-100) and polyoxyalkylene alkyl ether (NCW®-1002). Specifically, transient cavitation has been characterized through temporal variation of current measured during reduction of potassium ferricyanide at a 25 μm Pt microelectrode. The choice of surfactants and the megasonic frequency in this study was based on their wide applicability in integrated circuit (IC) fabrication [12,13].

2. Materials and methods

Potassium ferric cyanide ($K_3Fe(CN)_6$), potassium chloride (KCl), and Triton® X-100 were of reagent grade and procured from Sigma Aldrich. NCW®-1002 (10% aqueous solution) was purchased from Wako Pure Chemical Industries, Limited. High purity (99%) platinum (Pt) wires were obtained from Goodfellow. Experimental solutions were prepared using ultra pure deionized (DI) water of resistivity 18 MΩ-cm and contained 50 mM $K_3Fe(CN)_6$ and 0.1 M KCl without and with Triton® X-100 or NCW®-1002 surfactant added in the concentration range of 3E−3 to 125E−3% and

10E−3 to 100E−3% (by weight), respectively . Since oxygen reduction may interfere with measurements of ferricyanide reduction, care was taken to remove oxygen from the experimental solution by bubbling argon (Ar) gas for 30 min followed by keeping an Ar blanket over the solution. Oxygen removal from solutions was confirmed by measuring the oxygen content using an oxygen sensor (Rosemount Analytical model 499A DO).

Electrochemical experiments were performed using a three-electrode set-up consisting of a 25 μm diameter Pt disk as the working electrode and Pt wires of diameter 500 μm as counter and pseudo-reference electrodes. All electrodes were cleaned using iso-propyl alcohol, rinsed thoroughly with DI water, dried with N_2 blow and flame treated prior to each experiment. A ProSys® megasonic system consisting of a cylindrical tank (volume ∼500 ml) with ∼1 MHz circular transducer (area 22.2 cm²) was used for megasonic exposure of the experimental solution. The working electrode was positioned close to the center of the transducer at ∼2.0 cm above it. The details of the electrode set-up and the megasonic system appear elsewhere [12].

The megasonic field was applied either in a continuous or in a pulse mode. Fig. 1 shows schematically an example of continuous and pulse modes of sound propagation. Duty cycle specifies the percentage of the pulse period during which megasonic power is applied. In the continuous mode, the transducers are on continuously irrespective of the pulse period as the duty cycle is 100%. In the pulse mode, the on time of the transducers depends on the pulse period and duty cycle. For example, for a pulse period of 5 ms and duty cycle of 10%, the transducer will be on for 0.5 ms and off for 4.5 ms and this on/off cycle will continue for the entire megasonic exposure time. All experiments were run at 21 ± 2 °C and at a power density of 2.0 W/cm².

Chronoamperometry measurements were conducted using a Princeton Applied Research potentiostat PARSTAT® 2273 connected to an external oscilloscope NI USB-5133 which allowed acquisition of data at a sampling rate of 0.6–0.8 MHz. Measurements were first made for 5 s without application of potential and this was followed by a potential-step of −0.6 V (Vs Pt reference) and the current was recorded for ∼6 s. The potential-step
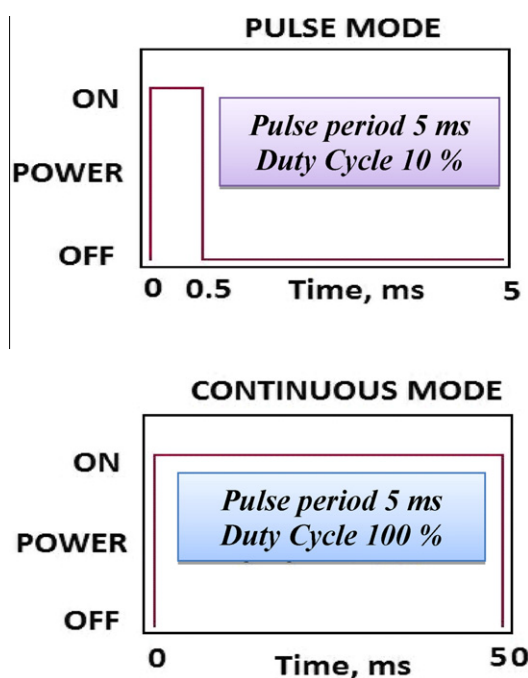

Fig. 1. A schematic showing continuous and pulse modes of sound propagation.

of −0.6 V was based on our preliminary measurements that showed complete reduction of ferricyanide occurs at this potential. After ~11 s, the transducer was turned on for 20 s, in either continuous (100% duty cycle, 5 ms pulse period) or pulse mode (10–40% duty cycle, 5 ms pulse period). The last few seconds of data were collected in the absence of megasonic field. The entire measurement lasted for about 40 s. National Instrument Labview 9.0 and DIAdem 2010 were used for data acquisition and graphical processing respectively.

3. Results and discussion

First part of the investigations was focused on characterization of cavitation behavior in the absence of any surfactants at different duty cycles. The effect of transducer duty cycle (for a given pulse period) on current is shown in Fig. 2a and d. The limiting current in the absence of megasonic field is ~0.3 μA and increases progressively with percent duty cycle in the presence of megasonic field. At 100% duty cycle, the limiting current is ~0.45 ± 0.05 μA. The increase in limiting current with the application of sound field may be attributed to increase in the flux of ferricyanide ions towards the electrode surface due to convective flow from acoustic streaming [14,15]. With decrease in the percent duty cycle, the transducer off time increases and it may be expected that the fluid streaming velocity reduces during this time due to viscous drag. As a result, the net fluid streaming velocity will be lower at smaller duty cycle, leading to a decrease in the limiting current.

During megasonic exposure, transient current 'peaks' (or actually 'inverse peaks') were observed to be riding on the limiting current for duty cycle from 25% to 100%. The rise and fall times of 'peaks' varied between 5–40 ms and 50–120 ms, respectively. The rise and fall of current refer to an increase and decrease of current magnitude, respectively, in the negative direction. Examples of

current 'peaks' with expanded time scale for 25% and 100% duty cycles are shown in Fig. 3. The frequency of occurrence and the magnitude of current 'peaks' increased with percent duty cycle. At 25% duty cycle , corresponding to transducer on-time of 1.25 ms for 5 ms pulse period, there were very few 'peaks' with a magnitude of ~0.3 μA or larger. With increase in duty cycle to 40 and 100%, the number of peaks with amplitude ⩾0.3 μA increased significantly. The occurrence of current peaks may be explained due to the collapse of transient cavities in the vicinity of the microelectrode. Such a collapse would concentrate ferricyanide ions at the liquid–vapor interface of the bubble [12]. Right after collapse, diffusion of ferricyanide towards the electrode surface would occur that will lead to varying concentration of ferricyanide at the microelectrode surface. The fact that the 'peaks' have a rise time of a few tens of milliseconds for transducer on (megasonic exposure) times of a few millisecond (1.25 ms and 2 ms) suggests that the 'peaks' are a result of an effect that continues even during the transducer off time. These results support that diffusion may well be the likely mechanism for the observed current 'peaks'.

It was discussed in our earlier paper [12] that the time scale of impact of microjetting ($\sim 10^{-7}$ s) is much smaller than the rise time of the current peaks observed in our experiments; however microjetting can still lead to a significant enrichment of ferricyanide species at the liquid–vapor interface due to considerable shrinkage of the collapsing cavity prior to the jet formation. While a jet may disperse some of the concentrated ferricyanide, diffusion is likely to be the dominant mechanism for the homogenization of the solution after asymmetric bubble collapse.

Fig. 4 shows root mean square (RMS) current as a function of time for different percent duty cycles. The RMS value of current at any given time was obtained by calculating root mean square of 10% (of total data length) of the current values on its either side. The choice of 10% was based on the fact that it allowed smoothing
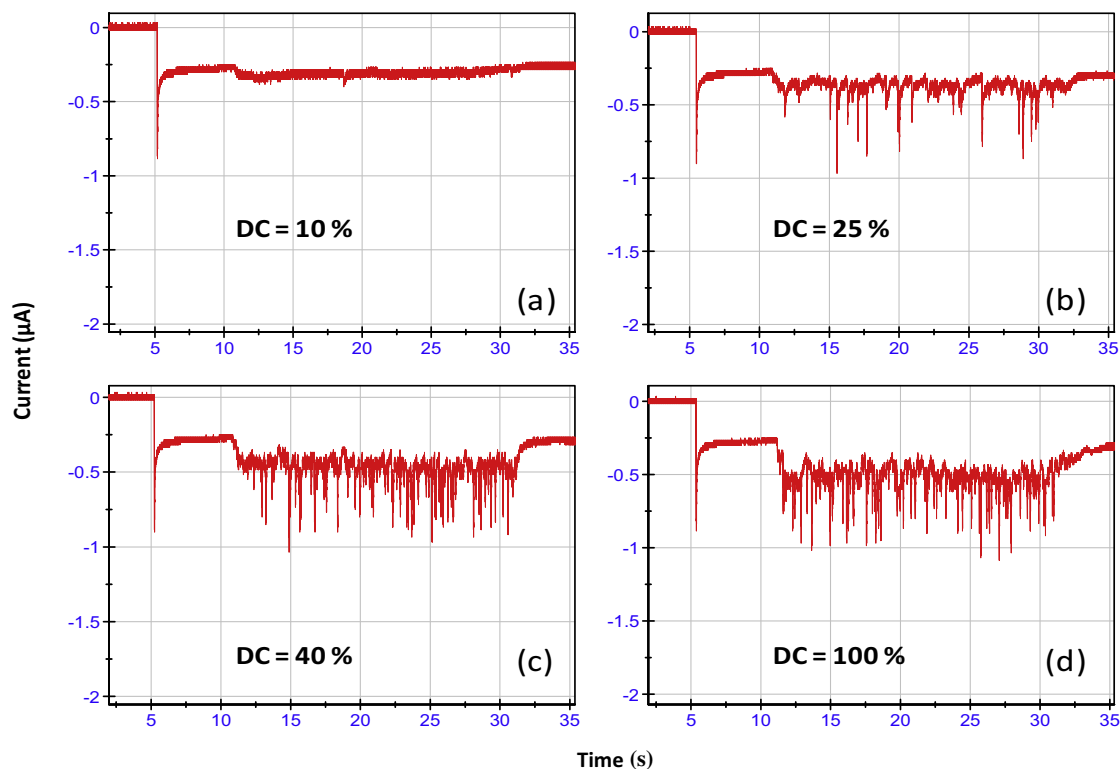

Fig. 2. Effect of acoustic duty cycle (total pulse length = 5 ms) on current during reduction of ferricyanide ions at 25 μm Pt microelectrode in Ar saturated aqueous solution containing 50 mM K₃Fe(CN)₆ and 0.1 M KCl (0–6 s = no applied potential and no megasonic irradiation, 6–11 s = applied potential of −0.6 V and no megasonic irradiation, 12–32 s = applied potential of −0.6 V and megasonic irradiation at ~1 MHz, ⩾33 s = applied potential of −0.6 V and no megasonic irradiation).
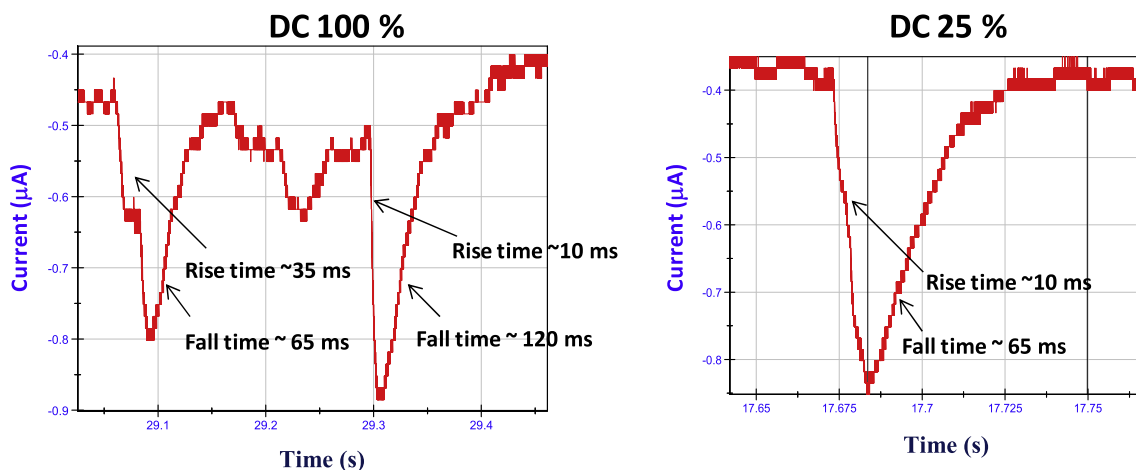
Fig. 3. Examples of current transients (with expanded time axis) obtained during megasonic exposure of Ar saturated aqueous solution containing 50 mM $K_3Fe(CN)_6$ and 0.1 M KCl.
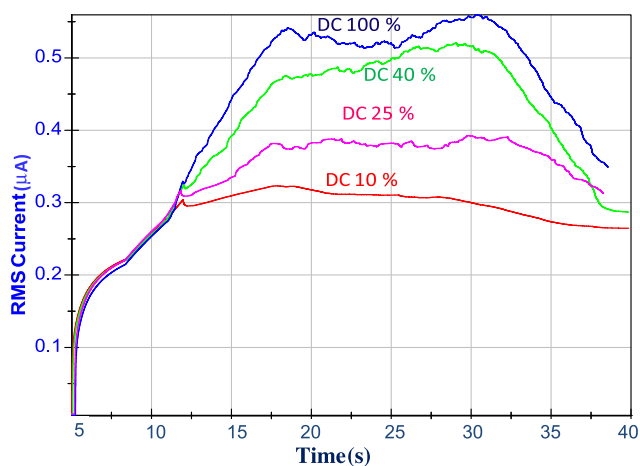

Fig. 4. Calculated root mean square (RMS) current as a function of time for different % duty cycle (total pulse length = 5 ms); Ar saturated aqueous solution containing 50 mM $K_3Fe(CN)_6$ and 0.1 M KCl ($\leqslant$6 s = no applied potential and no megasonic irradiation, 6–11 s = applied potential of -0.6 V and no megasonic irradiation, 12–32 s = applied potential of -0.6 V and megasonic irradiation at $\sim$1 MHz, $\geqslant$33 s = applied potential of -0.6 V and no megasonic irradiation).

of the current time curve so that comparison could be made between overall current at different percent duty cycles. The data from 6 to 11 s approximately represent the RMS values of current in the absence of megasonic field. During this period, all the curves overlay well over each other, as expected. The RMS current values in the megasonic exposure period of $\sim$12–32 s increase with increase in percent duty cycle. The data presented here clearly shows that total current due to acoustic streaming and transient cavitation increases with increase in percent duty cycle. The RMS current starts decreasing after 32 s for all cases as the megasonic energy was switched off after this time. Since these studies indicated that transient cavitation activity was highest at 100% duty cycle, the next step in the investigations was to explore the effect of surfactants at 100% duty cycle.

In order to understand the effect of Triton® X-100 and NCW®-1002 on transient bubble activity during megasonic exposure, chronoamperometry experiments were conducted using solutions containing different levels of the surfactant. The CMC (critical micelle concentration) of Triton® X-100 in aqueous solution containing up to 0.5 M of KCl has been reported to be in the range of 12E−3 to 16E−3% (0.20–0.25 mM) at $\sim$25 °C [16]. In this study,

four concentrations of Triton® X-100 were chosen, two below (3E−3 and 5.6E−3%) and two above (31E−3 and 125E−3%) the CMC. Similarly, the CMC of NCW®-1002, as reported by the manufacturer, is 50E−3% in aqueous solution and therefore experiments were conducted at surfactant concentrations of 10E−3, 30E−3 and 100E−3%.

The results for Triton® X-100 are shown in the form of chronoamperograms in Fig. 5. In the absence of megasonic field, at -0.6 V potential, the current is about 0.3 μA and is unaffected by the addition of the Triton® X-100 in the concentration range investigated. With the application of megasonic field, the streaming current increases to $\sim$0.45 ± 0.05 μA for all cases. Current transients were observed to be superimposed on the streaming current with their amplitudes and frequency of occurrences depending on the concentration of Triton® X-100 in the solution. The number of current 'peaks' with magnitude $\geqslant$0.3 μA in solution containing 3E−3% Triton® X-100 is slightly higher than that in solution with no surfactant. As the concentration of Triton® X-100 increases to 5.6E−3% and 31E−3%, the number of current 'peaks' with amplitude $\geqslant$0.3 μA further increases. The chronoamperogram for solution containing 125E−3% Triton® X-100 shows highest number of current 'peaks' with amplitude $\geqslant$0.3 μA compared to other solutions.

Fig. 6 illustrates RMS current as a function of time for solutions with varying levels of Triton® X-100. The RMS current values for time less than 11 s correspond to those under non-megasonic conditions and those $\geqslant$12 s are the ones obtained during megasonic exposure of the experimental solution. It may be seen that the RMS current for 3E−3% Triton® X-100 solution during megasonic exposure time period is about the same as that for solution with no surfactant. Increasing Triton® X-100 concentration to 125E−3% significantly increases the RMS current to $\sim$0.9 μA during the end of megasonic exposure.

In the case of NCW®-1002 aqueous solutions, the chronoamperometry results (shown in Fig. 7a and d) are similar to those observed for Triton® X-100 solutions. The baseline (no megasonic) and streaming current values were unaffected by presence of NCW®-1002 and were measured to be $\sim$0.3 and 0.45 μA, respectively. The current peaks due to transient cavitation, however, were strongly affected with surfactant addition. The frequency of occurrence of current peaks with amplitude $\geqslant$0.3 μA was significantly increased with the addition of NCW®-1002 at all concentrations in the range of 0.01–0.1%.

The chronoamperometry results for Triton® X-100 and NCW®-1002 clearly indicate that the addition of these non-ionic surfactants to aqueous solution increases the number of transient cavity
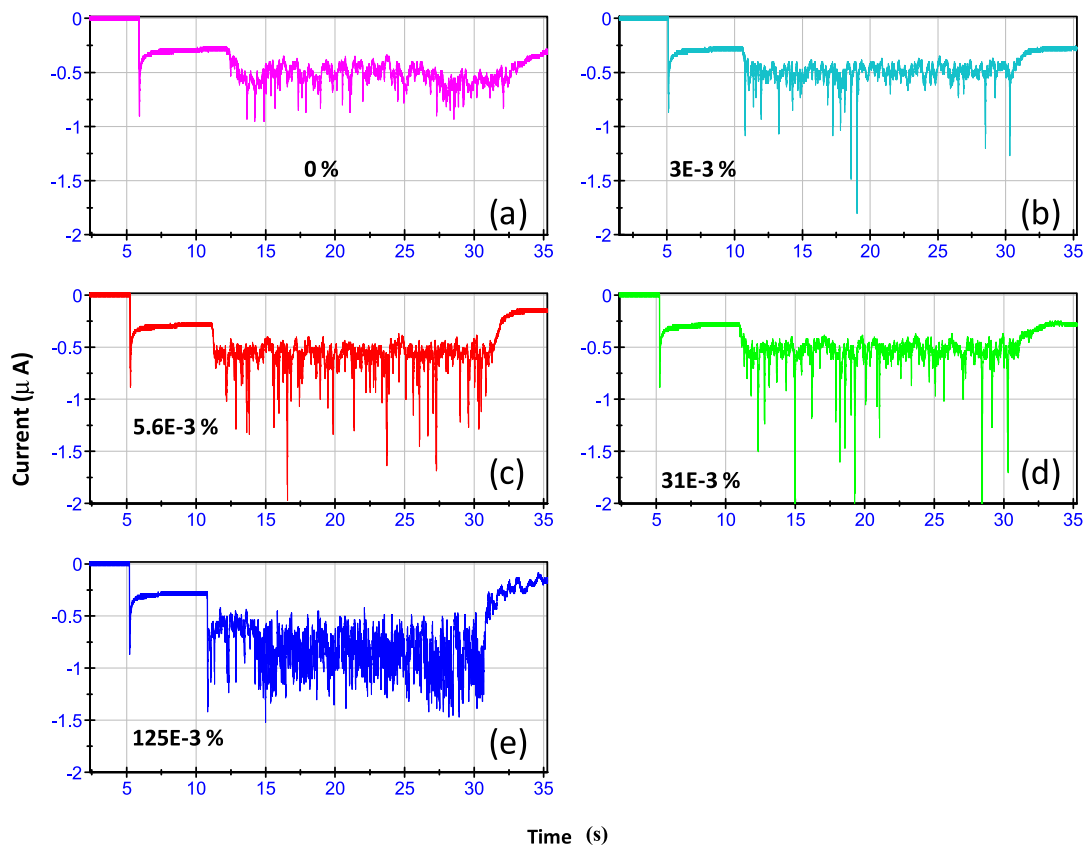
Fig. 5. Effect of Triton® X-100 concentration on current during reduction of ferricyanide ions at 25 μm Pt microelectrode in Ar saturated aqueous solution containing 50 mM K₃Fe(CN)₆ and 0.1 M KCl (pulse time 5 ms, duty cycle 100% during megasonic exposure; 0–6 s = no applied potential and no megasonic irradiation, 6–11 s = applied potential of −0.6 V and no megasonic irradiation, 12–32 s = applied potential of −0.6 V and megasonic irradiation at ∼1 MHz, ⩾33 s = applied potential of −0.6 V and no megasonic irradiation).
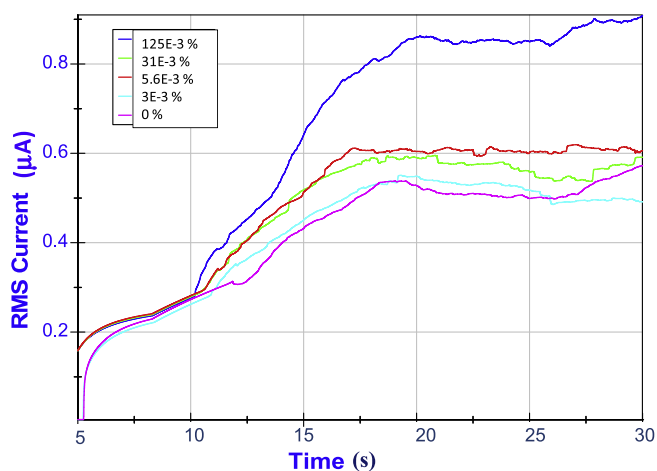

Fig. 6. Calculated root mean square (RMS) current as a function of time for Ar saturated aqueous solution (50 mM K₃Fe(CN)₆ and 0.1 M KCl) containing varying levels of Triton® X-100 (pulse time 5 ms, duty cycle 100% during megasonic exposure; ⩽6 s = no applied potential and no megasonic irradiation, 6–11 s = applied potential of −0.6 V and no megasonic irradiation, ⩾12 s = applied potential of −0.6 V and megasonic irradiation at ∼1 MHz).

collapses. The IC industry may use this characteristic feature of non-ionic surfactants to their advantage as higher cavitation activity needed for wafer cleaning can be achieved at a given transducer power density by using these surfactants.

Fig. 8 shows the maximum number of moles of ferricyanide transported (calculated from the area of the current transient) per unit area of the electrode surface in 20 s time frame due to combined streaming and transient cavitation as a function transducer duty cycle and surfactant addition. As can be clearly seen from the figure, the maximum number of moles of ferricynide transported to the electrode surface increases with the percent duty cycle and is highest when surfactant is added to the aqueous solution. Since the streaming current was unchanged with the addition of surfactant (as discussed earlier), the increase in transport of ferricyanide to the electrode surface in the presence of surfactants is predominantly due to more intense transient cavity collapse.

Keswani et. al., have shown that ferricyanide concentration, C_A, at different radial distances (r) and times (t) after the collapse of single transient cavity can be related to the amount (moles) of ferricyanide, M, accumulated at the liquid–vapor interface of the cavity at the end of its collapse using Eq. (1) [12]. The derivation for this equation is shown in Appendix A.

$$C_A = C_B + \frac{M}{8(\pi Dt)^{\frac{3}{2}}} e^{-\frac{r^2}{4Dt}} \tag{1}$$

In the above equation, C_B and D are the bulk concentration and the diffusivity of ferricyanide species in the solution, respectively.

Since current is proportional to the concentration of the electroactive species at the electrode surface [17,18], higher current peaks measured in the chronoamperogram would mean higher concentration of ferricyanide species at the electrode surface. With the addition of surfactant, although current peaks with higher amplitude were observed, the rise times were still in the same range (5–40 ms) as those in the absence of surfactant. Increase in the value of M in Eq. (1) would lead to higher C_A at a given distance (r) and time (t) *without changing the rise time of current*. Previously,
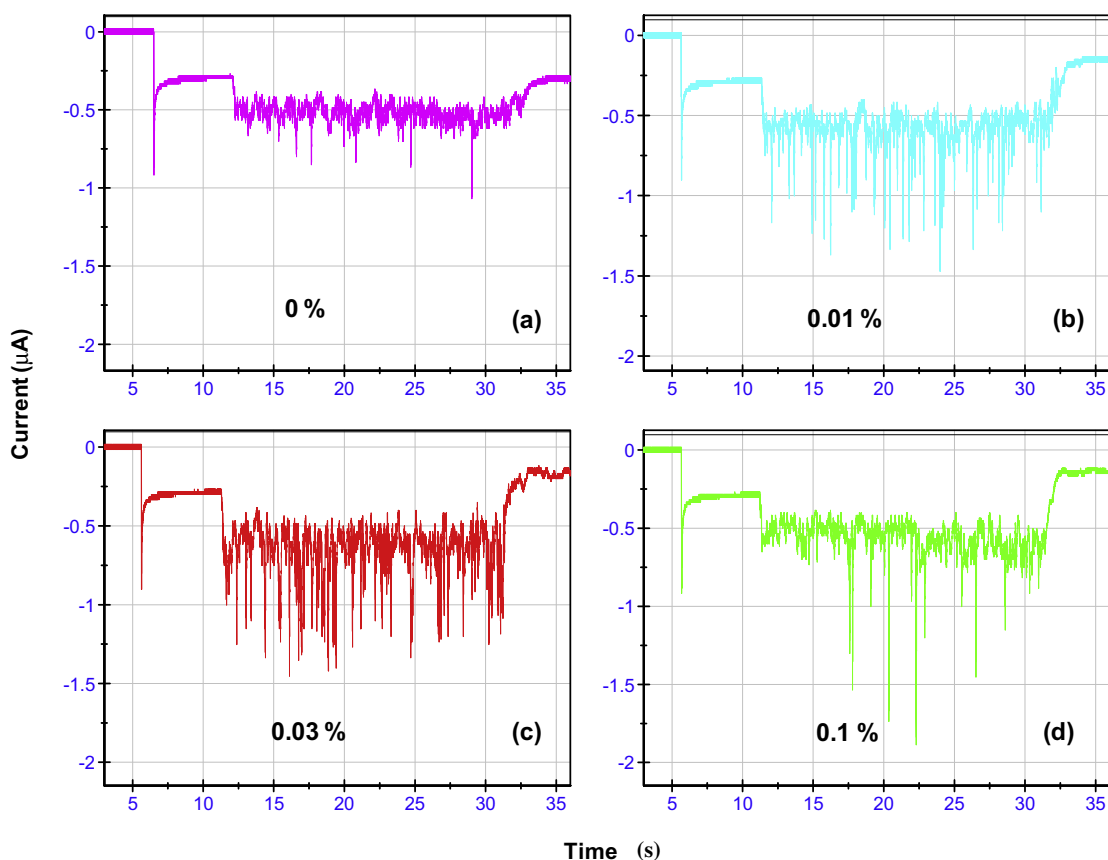
Fig. 7. Effect of NCW®-1002 concentration on current during reduction of ferricyanide ions at 25 μm Pt microelectrode in Ar saturated aqueous solution containing 50 mM K$_3$Fe(CN)$_6$ and 0.1 M KCl (pulse time 5 ms, duty cycle 100% during megasonic exposure; 0–6 s = no applied potential and no megasonic irradiation, 6–11 s = applied potential of −0.6 V and no megasonic irradiation, 12–32 s = applied potential of −0.6 V and megasonic irradiation at ∼1 MHz, ⩾33 s = applied potential of −0.6 V and no megasonic irradiation).
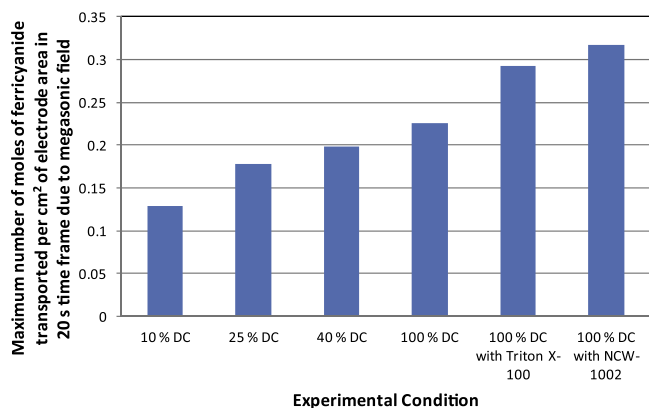

Fig. 8. Effect of duty cycle and addition of surfactant on maximum number of moles of ferricyanide transported per unit area of the electrode surface in 20 s time frame due to a megasonic field.

the authors of this paper have shown that M is related to the maximum size of the cavity just prior to its collapse [12]. In the absence of any surfactant, the maximum cavity radius and the range of distances between the center of collapsed cavity (where the ferricyanide concentrates) and the electrode surface were estimated to be ∼7 μm and 5–10 μm, respectively. These parameters were extracted by matching the concentration vs. time data (based on the model) with the shape of the current peaks obtained experimentally. Similar calculations performed in the case of surfactant solutions yielded maximum bubble radius of 12 μm (for high amplitude current peaks) and separation distance of 5–10 μm be-

tween the collapsed cavity and the electrode surface. It may be noted that it is quite possible for the maximum bubble radius to be larger than the distance between the collapsed cavity and the electrode surface. Indeed during collapse near a solid surface, the cavity deforms asymmetrically and its center of mass moves closer to the solid boundary as the collapse progresses [19]. Since, in Triton® X-100 and NCW®-1002 solutions, the measured peak currents were higher, it may be expected that individual bubbles in these solutions must also be of larger size than that in the solution without any surfactant. We believe that bubble growth by rectified diffusion is most likely improved in the presence of non-ionic surfactants such as Triton® X-100 and NCW®-1002 which results in the bubble population of larger size leading to more violent collapses.

Although, it may seem that our results for cavitation activity in the presence of Triton® X-100 are in contradiction with those in the paper by Stottlemyer et. al., the experimental conditions used for our experiments were quite different. They measured acoustic and SL emissions from a single air bubble (generated by either injecting air with a small syringe, or by locally boiling the water) in degassed solution *at an ultrasonic frequency of 16.5 kHz.* In the current work, electrochemical measurements were made in argon saturated aqueous solution for an argon bubble cavitating in a multi bubble environment *for a much higher sound frequency of ∼1 MHz.*

4. Conclusions

Characterization of transient cavitation in aqueous solutions of non-ionic surfactants irradiated with ∼1 MHz sound frequency was carried out using high resolution chronoamperometry. *In the*

absence of surfactants, the magnitude of the limiting current due to acoustic streaming and current 'peaks' due to transient cavitation increased with an increase in the percent duty cycle of megasonic field. *The addition of Triton® X-100 or NCW®-1002 to aqueous solutions* in the concentration range of ~3E−3 to 125E−3% (by weight) increased the frequency of occurrence of transient cavitation current 'peaks' with amplitudes $\geqslant$0.3 μA but did not have any effect on the streaming current. A mathematical analysis based on diffusion showed that the maximum cavity radius prior to collapse increases from 7 to 12 μm with the addition of surfactant to the aqueous solution. However, the separation distance (5–10 μm) between the center of collapsed cavity and the electrode surface was unaffected with the presence of surfactants.

Acknowledgements

Appendix A

If C_A is the concentration of ferricyanide at a distance r from the center of bubble after its collapse at any time t, then the differential equation in spherical coordinates can be written as:

$$D\frac{\partial}{\partial r}\left(4\pi r^2\frac{\partial C_A}{\partial r}\right)=4\pi r^2\frac{\partial C_A}{\partial t} \tag{A1}$$

where D, the diffusion coefficient of ferricyanide ion, is assumed to be independent of r

$$D\frac{\partial^2 C_A}{\partial r^2}+\frac{2D}{r}\frac{\partial C_A}{\partial r}=\frac{\partial C_A}{\partial t} \tag{A2}$$

Let $\overline{C_A}=C_A-C_B$
Eq. (A2) now becomes,

$$D\frac{\partial^2 C_A}{\partial r^2}+\frac{2D}{r}\frac{\partial \overline{C_A}}{\partial r}=\frac{\partial \overline{C_A}}{\partial t} \tag{A3}$$

Let $u=r\overline{C_A}$
Eq. (A3) can be written as

$$D\frac{\partial^2 u}{\partial r^2}=\frac{\partial u}{\partial t} \tag{A4}$$

Taking Laplace transform of Eq. (A4)

$$su_L(r,s)-u(r,t=0)=D\frac{\partial^2 u_L(r,s)}{\partial r^2} \tag{A5}$$

At $t=0, C_A=C_B,\ \overline{C_A}=0,\ u=0$

$$su_L(r,s)=D\frac{d^2 u_L(r,s)}{dr^2} \tag{A6}$$

Eq. (A6) is an ordinary differential equation and the solution to this equation is:

$$u_L=Ae^{-\sqrt{\frac{s}{D}}r}+Be^{\sqrt{\frac{s}{D}}r} \tag{A7}$$

As $r\to\infty, C_A\to C_B,\ \overline{C_A}\to 0, u\to 0$ and $u_L\to 0$. Therefore, B must be zero

$$u_L=Ae^{-\sqrt{\frac{s}{D}}r} \tag{A8}$$

If M is the moles of ferricyanide accumulated at $r=0$ at the end of transient cavity collapse, then

$$M=\int_0^\infty (C_A-C_B)4\pi r^2 dr \tag{A9}$$

$$M=4\pi\int_0^\infty urdr \tag{A10}$$

Taking Laplace Transform,

$$\frac{M}{s}=4\pi\int_0^\infty u_L rdr \tag{A11}$$

$$\frac{M}{s}=4\pi\int_0^\infty Ae^{-\sqrt{\frac{s}{D}}r}rdr \tag{A12}$$

After integration by parts,

$$A=\frac{M}{4\pi D} \tag{A13}$$

Therefore,

$$u_L=\frac{M}{4\pi D}e^{-\sqrt{\frac{s}{D}}r} \tag{A14}$$

Taking Laplace Inverse,

$$u=\frac{Mr}{8(\pi Dt)^{\frac{3}{2}}}e^{-\frac{r^2}{4Dt}} \tag{A15}$$

$$C_A=C_B+\frac{M}{8(\pi Dt)^{\frac{3}{2}}}e^{-\frac{r^2}{4Dt}} \tag{A16}$$

References

[1] A. Busnaina, G. Gale, Ultrasonic and megasonic particle removal, Proc. Precis. Clean. (1995) 347–359.
[2] P. Deymier, J. Vosseur, A. Khelif, B. Djafari-Rouhani, L. Dobrzynski, S. Raghavan, Streaming and removal forces due to second-order sound field during megasonic cleaning of wafers, J. Appl. Phys. 88 (11) (2000) 6821–6835.
[3] J. Park, S. Lee, S. Kim, Particle removal and its mechanism on hydrophobic silicon wafer in highly diluted NH$_4$OH solutions with an added surfactant, Jpn. J. Appl. Phys. 40 (11) (2001) 6182–6186.
[4] M. Ashokkumar, F. Grieser, The effect of surface active solutes on bubbles in an acoustic field, Phys. Chem. Chem. Phys. 9 (42) (2007) 5621–5728.
[5] W.W. Mansfield, Nature 175 (1955) 247–249.
[6] L. Crum, Measurements of the growth of air bubbles by rectified diffusion, J. Acoust. Soc. Am. 68 (1) (1980) 203–211.
[7] T. Oolman, H. Blanch, Bubble coalescence in stagnant liquids, Chem. Eng. Commun. 43 (1986) 237–261.
[8] L. Crum, Rectified diffusion, Ultrasonics 22 (5) (1984) 215–223.
[9] T. Stottlemyer, R. Apfel, The Effects of Surfactant Additives on the Acoustic and Light Emissions from a Single Stable Sonoluminescence Bubble, 102(3) (1997) 1418–1423.
[10] D. Sunartio, M. Ashokkumar, F. Grieser, Study of the coalescence of acoustic bubbles as a function of frequency, power, and water-soluble additives, J. Am. Chem. Soc. 129 (2007) 6031–6036.
[11] J. Lee, S. Kentish, T. Matula, M. Ashokkumar, Effect of surfactants on inertial cavitation activity in a pulsed acoustic field, J. Phys. Chem. B 109 (2005) 16860–16865.
[12] M. Keswani, S. Raghavan, P. Deymier, Characterization of transient cavitation in gas sparged solutions exposed to megasonic field, Microelectron. Eng. (2012), http://dx.doi.org/10.1016/j.mee.2011.11.013.
[13] Y. Xu, A. Michael, C. Kwok, Formation of ultra-smooth 45° Micromirror on (100) silicon with low concentration TMAH and Surfactant: Techniques for enlarging the truly 45° portion, Sensors Actuators A: Phys. 166 (1) (2011) 164–171.
[14] E. Maisonhaute, P. White, R. Compton, Surface acoustic cavitation understood via nanosecond electrochemistry, J. Phys. Chem. B 105 (48) (2001) 12087–12091.
[15] F. Marken, R. Akkermans, R. Compton, Voltammetry in the presence of ultrasound: the limit of acoustic streaming induced diffusion layer thinning and the effect of solvent viscosity, J. Electroanal. Chem. 415 (1996) 55–63.
[16] J. Molina-Bolivar, J. Aguiar, C. Ruiz, Light scettering and florescence probe studies on miscellar properties of Triton X-100 in KCl solutions, Mol. Phys. 99 (20) (2001) 1729–1741.
[17] B. Pollet, J. Hihn, M. Doche, J. Lorimer, A. Mandroyan, T. Mason, Transport limited currents close to an ultrasonic horn: equivalent flow determination, J. Electrochem. Soc. 154 (10) (2007) E131–138.
[18] S. Hwang, PhD Dissertation, Integrated CMOS Microsystems for Electrochemical Sensing, 2010.
[19] E. Brujan, T. Ilkeda, Y. Matsumoto, Jet formation and shock wave emission during collapse of ultrasound-induced cavitation bubbles and their role in the therapeutic applications of high-intensity focuses ultrasound, Phys. Med. Biol. 50 (2005) 4797–4809.